Developing a trilayer processing technique for superconducting Y $Ba_2Cu_3O_{7-\delta}$ thin films by using Ge ion implantation

2005 Supercond. Sci. Technol. 18 477

(http://iopscience.iop.org/0953-2048/18/4/016)

INSTITUTE OF PHYSICS PUBLISHING SUPERCONDUCTOR SCIENCE AND TECHNOLOGY

Supercond. Sci. Technol. **18** (2005) 477–481 doi:10.1088/0953-2048/18/4/016

Developing a trilayer processing technique for superconducting $YBa_2Cu_3O_{7-\delta}$ thin films by using Ge ion implantation

I Avci[1,2,4], M Tepe[2], B Oktem[1], U Serincan[3], R Turan[3] and D Abukay[1]

[1] Department of Physics, Izmir Institute of Technology, 35437-Urla-Izmir, Turkey
[2] Department of Physics, Ege University, 35100 Bornova, Izmir, Turkey
[3] Department of Physics, Middle East Technical University, 06531 Ankara, Turkey

E-mail: ilbeyiavci@iyte.edu.tr

Received 22 June 2004, in final form 6 December 2004
Published 21 February 2005
Online at stacks.iop.org/SUST/18/477

Abstract

For making trilayer superconducting devices based on $YBa_2Cu_3O_{7-\delta}$ (YBCO) thin film processing, we developed a new technique by employing Ge ion implantation. A YBCO thin film of 150 nm thickness having high *c*-axis orientation and a transition temperature, T_c, of 90 K was implanted with 80 keV, 1×10^{16} Ge ions cm^{-2} at room temperature. By the result of TRIM calculation, Ge ions were found to penetrate into the YBCO thin film approximately 60 nm below the surface of the film, thus leaving the lower part of the film as a superconductor. Upon implantation with Ge ions, the implanted upper part of the sample lost its electrical conductivity and diamagnetism while its original crystalline structure was preserved. The implanted ions we found did not alter the overall crystal structure of the YBCO thin film; this allowed us to grow an epitaxial superconducting upper layer of YBCO on top of the implanted area, leaving no need to use any buffer layer. The superconducting properties of the upper layer were similar to those of the pure YBCO base layer with an increased room temperature resistivity and a lowered T_c (88 K). This process provides an effective method for fabrication of a trilayer HTS device structure.

(Some figures in this article are in colour only in the electronic version)

1. Introduction

In superconducting electronics, high-T_c YBCO thin films have been widely used as processing materials for device fabrication. The processing of YBCO thin films as Josephson junctions and SQUIDs, constructed vertically on a substrate, has been reserving an important place in the multilayer fabrication [1–6]. There is a demand for multilayer fabrication for the purpose of reducing the noise problems and improving the sensitivity of these devices [7–9]. This, however, requires use of some complicated fabrication techniques such as buffer layer construction between the superconducting YBCO layers.

[4] Address for correspondence: Department of Physics, Izmir Institute of Technology, 35437-Urla-Izmir, Turkey.

The progress in HTS device technology and the increasing complexity of HTS circuitry continues to push the limits of the materials and the processes used to fabricate multilayer devices. Devices require the superconducting layers separated with insulating or semiconducting layers grown epitaxially without degradation of their superconducting parameters. This can be quite difficult to achieve in practice due to the planar geometry inherent in these devices. For the multilayer device fabrication in semiconductor technology, ion implantation has commonly been in use for last few decades. In high temperature superconducting materials, the ion implantation technique has been used for modifying the structure and improving some critical parameters of superconductors with various types of ions [10–20]. The

idea of using the ion implantation technique with suitable ion energy and dose for the purpose of creating an insulating layer serving as a separator between the superconducting layers was the main motive of this work. In our previous work, we presented the growth of a bilayer YBCO structure with Si ion implantation [21]. In that study, upon Si ion implantation, the base layer YBCO thin film completely lost its superconductivity and became a semiconductor. Thus, a semiconductor–superconductor junction has been obtained by the growth of a second superconductor YBCO layer on top of the implanted area. In the ion implantation process, the main problem which has to be taken into account is the redistribution of the implanted ions after subsequent annealing and/or epitaxial growth. A study of the redistribution of the implanted Ge ions and their diffusion mechanisms depending on the thermal annealing in semiconductors has been performed by Turan *et al* [22]. They reported that the ion redistribution was asymmetric and the diffusion of Ge in Si was mostly towards the surface with smaller diffusion constant. Although the mechanism of the ion redistribution is unknown, further study of this subject may shed light on unsolved problems of the growth-enhanced diffusion of dopants in YBCO. In this work, we have looked to obtain a trilayer structure on superconducting YBCO thin film by implanting Ge ions with the anticipation of obtaining an insulating layer formed at the surface of the base layer of YBCO, hence eliminating the need for buffering.

2. Experimental details

For the fabrication of the trilayer device, $10 \times 10 \times 0.5$ mm^3 (100)-cut MgO single-crystal substrates were used. The YBCO layers were deposited onto the substrate by using the DC inverted cylindrical magnetron sputtering (ICMS) technique. The temperature of the sample holder was 800 °C, the partial pressure of the Ar gas was 0.5 mbar and the partial pressure of O_2 gas was 0.1 mbar. The resulting layers having 150 nm thicknesses were found to have full *c*-axis orientation and their full width at half maximum (FWHM) value of the rocking curve of (005) peak was measured as $\leqslant 0.22°$.

The first layer serving as the base layer was Ge ion implanted by exposing its surface across a metal mask, to a beam of energy of 80 keV and a dose of 1×10^{16} Ge-ions cm^{-2} at room temperature. The beam current density was about 0.3 μA cm^{-2}. The contact pads evaporated onto the base layer are protected from the ion beam by using a metal mask. The ion distribution was estimated by the computer simulation program TRIM [23], which is realistic with respect to the experiment.

After the implantation process, the sample, prior to the deposition of YBCO for the second layer, was heated to 800 °C, gradually increasing the power of the heater in the sputtering chamber, keeping the same gas mixture at the same pressure as for the first sputtering process. This step was completed in 45 min. This heat treatment may cause a diffusion of Ge ions across the interface between the base layer and the implanted zone within the film. The deposition of a second layer film having 150 nm thickness was completed in 90 min. During this process, the small amount of Ge diffusion may occur across the interface between the implanted zone and the second layer.

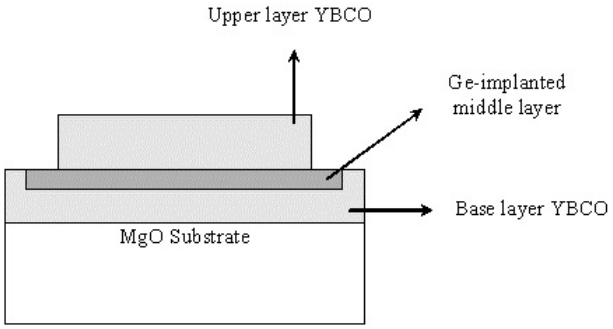

Figure 1. Schematic cross-section of YBCO/implanted Ge ions/ YBCO trilayer device.

Characterization of the sample before and after each step of the processing has been done by employing resistance–temperature (R–T), ac magnetic susceptibility versus temperature (χ–T), x-ray diffraction analysis (XRD) and atomic force microscopy (AFM). The resistive transition curves were obtained by using the four-point method. The ac susceptibility measurement was carried out by using the mutual inductance method with the excitation field of $h(t) = h_0 \sin 2\pi f t$ where $f = 1$ kHz and $h_0 = 18.5$ A m^{-1}. The crystal structure and the contact mode surface morphology were determined by XRD and AFM.

3. Results and discussion

Figure 1 shows a sketch of the final structure we want to fabricate. The YBCO base layer was sputtered first onto the substrate, and then implanted with Ge ions through the mask which was used to leave a space a few millimetres wide at the edges of the film for placing the contact pads onto the base layer. Finally, upper layer YBCO film was deposited onto the implanted area through another mask which was used to leave a space a few millimetres wide at the edges of the implanted area for placing the contact pads onto the middle layer.

Before the ion implantation process we carried out a TRIM simulation to estimate the penetration profile of the ions and the necessary ion energy for the YBCO thin film. In order to form a non-superconducting zone within the film which extends down to a depth from the surface of the film, the energy of the Ge ions was chosen as 80 keV with a dose of 1×10^{16} Ge ions cm^{-2} at room temperature. The result of the simulation has produced a depth profile for Ge ions in YBCO which is shown in figure 2 and the penetration depth was estimated as 60 nm below the surface of the film.

The implanted layer was expected to behave as non-superconducting because of an increased density of defects produced after the impact of Ge ions with the atoms of *c*-axis YBCO film. The results of both real and imaginary parts of ac magnetic susceptibility measurements of the sample (χ–T) are given in figure 3. The unimplanted, pure YBCO film has shown a rather sharp transition at the temperature of 91 K with a transition width of $\Delta T \sim 0.5$ K. The sharpness of the transition indicates the high quality of the obtained YBCO film. After Ge ion implantation the sample has shown superconductivity with a depressed transition temperature of 88 K. As seen from figure 3, the diamagnetic saturation of

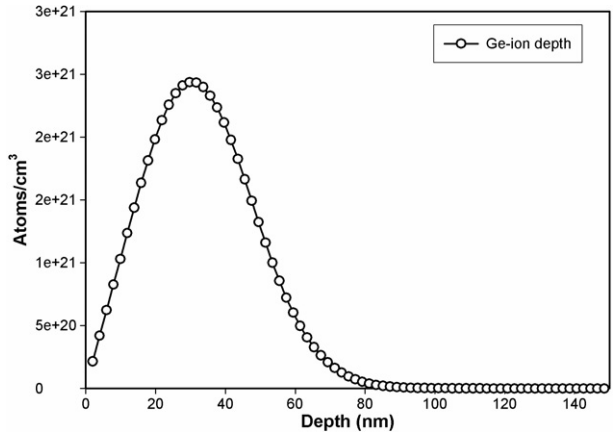

Figure 2. TRIM depth profile of Ge ion implantation into the YBCO thin film.

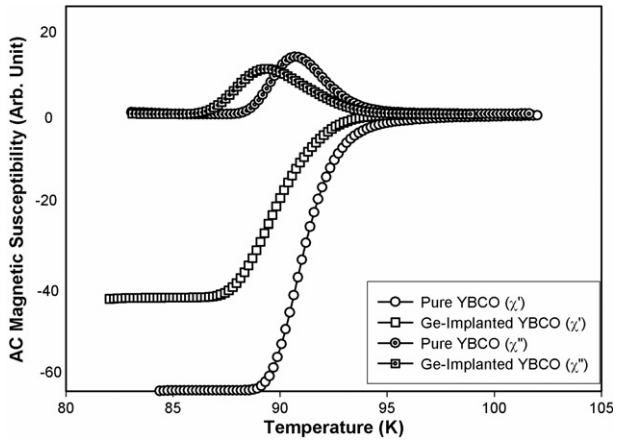

Figure 3. Ac magnetic susceptibility–temperature characteristics of pure and Ge ion implanted YBCO thin films.

the Ge ion implanted sample has decreased to a lower value compared with that of the unimplanted one. The difference in diamagnetic saturation values can be related to the volume of the superconductor. Therefore, it can be said that the volume of the superconductor has reduced after implantation. Here we may conclude that the implanted Ge ions have created a non-superconducting zone just below the surface and the rest of the film has remained superconducting, hence forming a two-layer structure within the bulk of the film. The depression of the transition temperature appearing in the ac susceptibility measurement is thought to stem from the formation of the stress field on the lower superconducting part due to the implanted layer above it.

In the literature to our knowledge not much is known about the diffusion of Ge in YBCO, hence we are not able to speculate to what extent this has occurred during both the annealing stage after implantation and the heating stage while depositing the second layer of YBCO on top of the implanted part. It may also be expected that some crystal defects which occurred during the implantation might have been removed, at least partially, during these heat treatments.

The XRD results of the pure and implanted samples are shown in figure 4. The full width at half maximum (FWHM) values are measured, before and after the implantation, from rocking curves on the YBCO(005) peaks of sample as

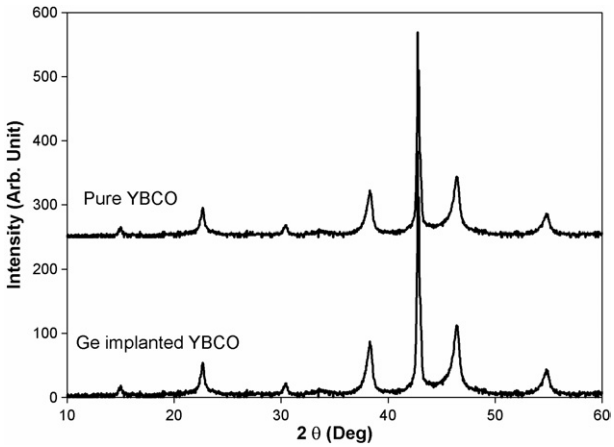

Figure 4. XRD patterns of pure and Ge ion implanted YBCO thin films.

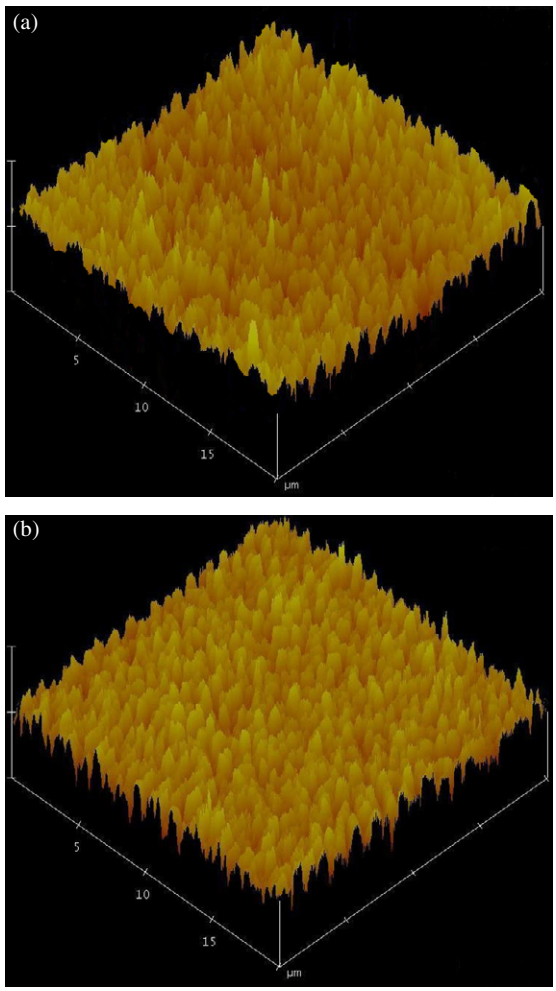

Figure 5. AFM surface morphologies of pure (a) and Ge ion implanted (b) samples.

about 0.22°, indicating high *c*-axis orientations of the film. Interestingly, no variations are observed in the positions of the peaks in the XRD results, which indicates that Ge ion implantation did not result in any significant change in the crystal structure of the sample.

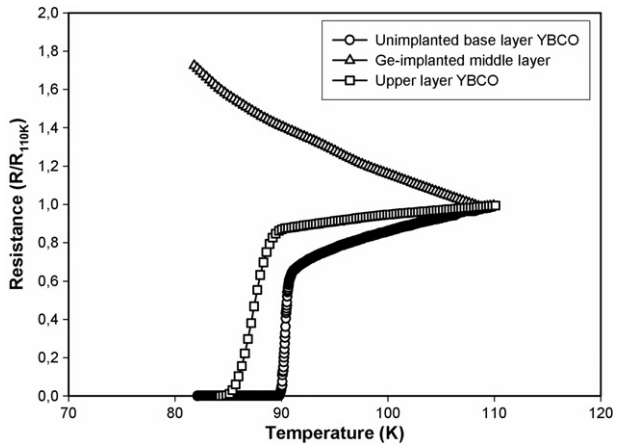

Figure 6. Resistance–temperature measurements of individual layers of a YBCO/implanted Ge ions/YBCO trilayer device.

The surface morphology of the sample before and after implantation was characterized by atomic force microscopy (AFM) and the results are shown in figures 5(a) and (b). The mean roughness, R_a, within a scanned area of 20 × 20 μm^2 was measured as about 5 nm for the pure sample which is a characteristic value of dc sputtered YBCO films, and an R_a value of 12 nm was measured on the surface of the implanted region within the same scanned area. The large difference between these two values shows that the Ge ion implantation has strongly affected the surface morphology of the layer.

The $R(T)$ measurement on the bottom layer and upper layer of YBCO were carried out over the contacts placed on the corresponding layers independent of each other; i.e. the superconducting layer and the ion implanted region have no common input for the measuring current. Another way of saying this is that there were no parallel conducting channels for the measuring current input during the $R(T)$ measurements over these layers. The results of resistance measurements are shown in figure 6. The normal state resistance values are about 100 Ω for the base layer, about 160 Ω for the top layer and 4 MΩ for the intermediate layer. Because of these large differences in normal state resistances between layers, the graphs should be drawn in normalized form for clear comparison. The resistance behaviour of the Ge ion implanted intermediate layer was significantly similar to that of a semiconductor, increasing with decreasing temperature. The resistance behaviour of the upper and the bottom layer YBCO has shown a typical superconducting transition. The transition width of the bottom layer was narrower than the upper layer and their descending slopes were also different from each other, namely the slope of the upper layer was less steep than that of the bottom layer. Although we tried to keep the deposition conditions the same for both layers during the sputtering process, the differences are quite visible from both curves, indicating the influence of the surface morphology of the implanted layer and the disturbed oxygen stoichiometry in the upper layer. In addition, one may expect some amount of diffusion of Ge ions from the implanted surface to the upper layer YBCO during its deposition, since the substrate temperature was increased up to 800 °C and stayed there for about 2 h.

The surface morphology of the top layer YBCO thin film was analysed by AFM and the results are given in figure 7. In the scanned area of 20 × 20 μm^2, the R_a value was measured as 12 nm which is the same value as that of the implanted surface. This observation gives support to the idea that the upper layer was influenced by the morphology of the bottom layer, hence causing a broadening in the resistive transition as well as its slope. The grain sizes were found to vary around 1 μm and they follow a unidirectional elongation across the scanned surface, as viewed on the micrograph (see figure 7).

4. Conclusion

We have presented the fabrication of trilayer superconducting YBCO thin film structure by Ge ion implantation. According to the XRD analyses, Ge ion implantation does not affect the crystalline structure of the YBCO thin film. This allows the growth of a second layer superconducting YBCO film on top of the implanted area. With the employment of the passivation of the Ge implanted layers for improving the interface properties

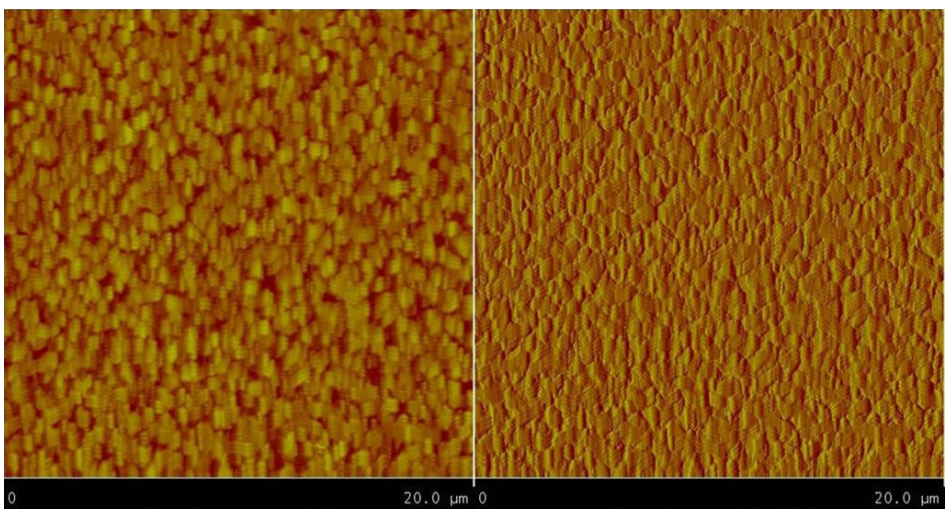

Figure 7. AFM surface morphology of the top layer YBCO thin film.

and solving the Ge diffusion mechanisms between the layers, this technique could be extended into a multilayer process for Josephson-junction-based electronic device production.

Acknowledgments

This study was supported by TUBITAK under the project number of TBAG-1272. The authors would like to express their gratitude to specialists at the Material Research Centre at Izmir Institute of Technology for their valuable suggestions in the analysis of AFM and XRD.

References

[1] Mahajan S, Ito W, Cho C H and Morishita T 1994 *Physica* C **220** 227–32
[2] Takeuchi I, Trajanovic Z, Peng J L, Li Z Y, Warburton P A, Lobb C J and Venkatesan T 1995 *Appl. Phys. Lett.* **66** 1824–6
[3] Li H Q, Ono R H, Vale L R, Rudman D A and Liou S H 1996 *Appl. Phys. Lett.* **69** 2752–4
[4] Merkle K L, Huang Y, Rozeveld S, Char K and Moeckly B H 1999 *Micron* **30** 539–59
[5] Shimakage H, Ono R H, Vale L R, Uzawa Y and Wang Z 2001 *Physica* C **357–360** 1416–9
[6] Lim H R, Kim D H, Kim I-S, Park Y K and Park J-C 2000 *Supercond. Sci. Technol.* **13** 1046–50
[7] Clarke J 1997 *Curr. Opin. Solid. State Mater.* **2** 3–10
[8] Takashima H, Kasai N and Shoji A 2003 *Physica* C **392–396** 1367–72
[9] Exon N J, Keene M N, Satchell J S, Chev N G, Wooliscroft M J, Lander K and Humphreys R G 1998 *Appl. Supercond.* **6** 663–7
[10] LaGraff J R, Pan G Z and Tu K N 2000 *Physica* C **338** 269–83
[11] Kahlmann F, Engelhardt A, Schubert J, Zander W, Buchal Ch and Hollkott J 1999 *Nucl. Instrum. Methods* B **148** 803–6
[12] Kuhn M, Schey B, Klarmann R, Biegel W, Stritzker B, Eisenmenger J and Leiderer P 1998 *Physica* C **294** 1–6
[13] Kilner J A and Li Y 1998 *Nucl. Instrum. Methods* B **139** 108–19
[14] Liu X T, Lu H X, Liu X H, Chen Q S and Pan S M 1997 *Physica* C **282–287** 2547–8
[15] Nan H Y, Yao X, Murakami M and Tanaka S 1997 *Physica* C **282–287** 1043–4
[16] Kato H, Kulpa A, Wong A, Hui D, Jaeger N A F, Carolan J F and Hardy W N 1997 *IEEE Trans. Appl. Supercond.* **7** 1616–9
[17] Hong S H, Baniecki J D, Ma Q Y, LaGraff J R and Murduck J M 1998 *Supercond. Sci. Technol.* **11** 375–7
[18] Kang D-J *et al* 2002 *Appl. Phys. Lett.* **80** 814–6
[19] Civale L, Marwick A D, Worthington T K, Kirk M A, Thompson J R, Krusin-Elbaum L, Sun Y, Clem J R and Holtzberg F 1991 *Phys. Rev. Lett.* **67** 648–51
[20] Konczykowski M, Rullier-Albenque F, Yacoby E R, Shaulov A, Yeshurun Y and Lejay P 1991 *Phys. Rev.* B **44** 7167–70
[21] Avci I, Tepe M, Serincan U, Oktem B, Turan R and Abukay D 2004 *Thin Solid Films* **466** 37–40
[22] Turan R and Finstad T G 1992 *Semicond. Sci. Technol.* **7** 75–81
[23] Ziegler J F 1996 *SRIM* (Yorktown Hights, NY: IBM Research)